Temporal evolution of plutonium concentrations and isotopic ratios in the Ukedo - Takase Rivers draining the Difficult-To-Return zone in Fukushima, Japan (2013–2020)

Aurélie Diacre, Thomas Chalaux-Clergue, Soazig Burban, Caroline Gauthier, Amélie Hubert, Anne-Claire Humbert, Irène Lefevre, Anne-Laure Fauré, Fabien Pointurier, Olivier Evrard

Angaben zur Veröffentlichung / Publication details:

Diacre, Aurélie, Thomas Chalaux-Clergue, Soazig Burban, Caroline Gauthier, Amélie Hubert, Anne-Claire Humbert, Irène Lefevre, Anne-Laure Fauré, Fabien Pointurier, and Olivier Evrard. 2023. "Temporal evolution of plutonium concentrations and isotopic ratios in the Ukedo - Takase Rivers draining the Difficult-To-Return zone in Fukushima, Japan (2013–2020)." Environmental Pollution 319: 120963. https://doi.org/10.1016/j.envpol.2022.120963.

Temporal evolution of plutonium concentrations and isotopic ratios in the Ukedo - Takase Rivers draining the Difficult-To-Return zone in Fukushima, Japan (2013–2020)☆

Aurélie Diacre [a,b,*], Thomas Chalaux Clergue [b], Soazig Burban [a], Caroline Gauthier [b], Amélie Hubert [a], Anne-Claire Humbert [a], Irène Lefevre [b], Anne-Laure Fauré [a], Fabien Pointurier [a], Olivier Evrard [b]

[a] Commissariat à L'Energie Atomique et Aux énergies Alternatives (CEA, DAM, DIF), F-91297, Arpajon, France
[b] Laboratoire des Sciences Du Climat et de L'Environnement (LSCE/IPSL), Unité Mixte de Recherche 8212 (CEA/CNRS/UVSQ), Université Paris-Saclay, Gif-sur-Yvette, France

A B S T R A C T

In 2011, the Fukushima Dai-Ichi Nuclear Power Plant (FDNPP) accident released significant quantities of radionuclides into the environment. Japanese authorities decided to progressively reopen the Difficult-To-Return Zone after the decontamination of priority reconstruction zones. These areas include parts of the initially highly contaminated municipalities located to the north of the FDNPP, including Namie Town, an area drained by the Ukedo and Takase Rivers. Eleven years after the accident, research focused on the spatial distribution of plutonium (Pu) and radiocesium (Cs) isotopes at contrasted individual locations. To complement previous results, the current research was conducted on flood sediment deposits collected at the same locations after major flooding events during eleven fieldwork campaigns organised between 2013 and 2020 at the outlet of the Ukedo and Takase Rivers (n = 22).

The results highlighted a global decrease of the Pu and ^{137}Cs contents in sediment with time during the abandonment phase in the region, from 2013 (238.20 fg g^{-1}) to 2020 (4.28 fg g^{-1}). Furthermore, based on the analysis of the ^{240}Pu/^{239}Pu isotopic ratios, the plutonium transiting these rivers (range: 0.166 – 0.220) essentially originated from the global fallout (0.180 ± 0.014 (Kelley et al., 1999)). Sediment showed contrasted properties in the two investigated rivers, which is likely mainly the result of the occurrence of Ogaki Dam on upper sections of the Ukedo River as it strongly impacts the material supply from this river to the Pacific Ocean. A statistical analysis highlighted the strong correlation between Pu activity concentrations and ^{137}Cs activities in both rivers, confirming that both radionuclides are transported with a similar pathway. Despite it was detected early after the accident (2011–2013), the current research demonstrates that plutonium originating from FDNPP is no longer detected in these rivers draining the Difficult-To-Return Zone at the onset of the reopening of the area to its former inhabitants.

1. Introduction

Following the accident that occurred at Fukushima Dai-Ichi Nuclear Power Plant (FDNPP) on March 11, 2011, large quantities of radionuclides were emitted into the environment, with a total activity estimated to 520 PBq, which deposited mainly in regions of Northeast Japan (Steinhauser et al., 2014). Models showed that ~ 80 % of radionuclide releases occurred over the ocean (Mathieu et al., 2018; MEXT, 2011). These emissions mainly consisted in volatile or semi-volatile fission products (^{137}Cs, ^{134}Cs, ^{131}I, …) although amounts of actinides (U, Pu) from the reactor fuel were also released (Steinhauser et al., 2014). The most significant contaminant released into the environment was radiocesium ($^{134+137}$Cs), with initial emissions estimated to 10 PBq of ^{137}Cs (Onda et al., 2020). In contrast, the releases of $^{239+240}$Pu were estimated

☆ This paper has been recommended for acceptance by Hefa Cheng.
* Corresponding author. Commissariat à l'Energie Atomique et aux énergies alternatives (CEA, DAM, DIF), Chemin du ru, 91297, Arpajon, France.
E-mail address: aurelie.diacre@lsce.ipsl.fr (A. Diacre).

to range from 1 GBq to 3.5 GBq, i.e. one million times lower than for radiocesium (Schneider et al., 2013; Shinonaga et al., 2014; Yamamoto et al., 2014; Zheng et al., 2013). From 2011 onwards, scientists focused on the characterization of the spatial distribution of radioactive fallout as a prerequisite to investigate the potential health and environmental impacts of this accident (Adachi et al., 2013; Aliyu et al., 2015; Evrard et al., 2015, 2013; Onda et al., 2020). The primary means of radiocesium transport where shown to be soil erosion and transfer of particle-bound radiocesium in river systems. In the case of actinides, some studies demonstrated their occurrence in the environment under the form of microparticles (Igarashi et al., 2019; Kurihara et al., 2020; Martin et al., 2019, 2016; Ochiai et al., 2018). Nevertheless, results suggest that their transportation in rivers may follow similar pathways as radiocesium (Evrard et al., 2014). At the *bulk* scale, research on the actinide isotopic characterization in sediment has shown that the $^{235}U/^{238}U$ does not allow to discriminate its source (Jaegler et al., 2019), which justifies the need to analyse Pu atom ratios to characterize its origin (Cao et al., 2016; Evrard et al., 2014; Jaegler et al., 2018; Johansen et al., 2021; Oikawa et al., 2015; Schneider et al., 2013; Shinonaga et al., 2014; Yamamoto et al., 2014). In particular, $^{240}Pu/^{239}Pu$ and $^{241}Pu/^{239}Pu$ isotopic ratios are powerful tools to identify the plutonium source. In the northern hemisphere, the main Pu source is linked to the atmospheric nuclear weapon tests performed from 1945 to 1980 (Bu et al., 2015a; Danesi et al., 2008; Muramatsu et al., 2001; Yamamoto et al., 2002). During this period, plutonium isotopes were globally spread in the stratosphere and they can be detected since then in the environment all around the world. The $^{240}Pu/^{239}Pu$ isotopic ratio of the global fallout in the Northern Hemisphere is estimated to 0.180 (± 0.014) (Kelley et al., 1999). Since the atmospheric nuclear tests, other emissions of plutonium into the environment occurred as a result of the Chernobyl Nuclear Power Plant and the FDNPP accidents. A specific labelling of soils in Northern Japan with the FDNPP Pu isotopic signature has also been outlined (Zheng et al., 2013). The plutonium isotopic composition in the fuel of FDNPP at the moment of the accident was reconstructed by Nishihara et al. (2012) based on model simulations. The $^{240}Pu/^{239}Pu$ isotopic ratio was shown to vary depending of the reactor of emission, with values of 0.339, 0.315 and 0.351, for reactors 1, 2 and 3, respectively.

As highlighted by Wu et al. (2022), only few studies investigated the Pu signature in sediment samples. These studies demonstrated the occurrence of specific Pu fallout due to FDNPP in samples collected between 2011 and 2013 (Evrard et al., 2014; Jaegler et al., 2019; Schneider et al., 2013; Steinhauser et al., 2015; Yamamoto et al., 2014) although, to the best of our knowledge, longer-term records and analyses on samples collected more recently near the FDNPP have not been conducted to detect potential further changes in these Pu signatures.

Accordingly, the objective of this study is to investigate the temporal changes in Pu signatures between 2013 and 2020 in flood sediment deposits collected in the Ukedo and the Takase Rivers draining a part of the Difficult-to-Return Zone, in Fukushima Prefecture, and to identify potential factors controlling these changes. To this end, the current research focused on (1) the characterization of the Pu activity concentrations in sediment and their evolution, (2) the potential changes in sediment Pu isotopic signatures within and between rivers throughout time, and (3) the identification of the potential control factors of the Pu activity concentrations and signatures using a simple statistical approach. This represents to the best of our knowledge the first decadal time series of Pu analyses in river sediment samples collected at the same locations within the Difficult-To-Return (DTR) Zone since the FDNPP accident.

2. Materials and methods

2.1. Study region

This study was conducted in the Ukedo River catchment located to the north of the FDNPP and draining a surface area of 534.8 km^2. It may be subdivided into two sub-catchments, i.e. Ukedo branch (201.6 km^2) and Takase branch (333.2 km^2). The Ukedo and Takase catchments are mainly covered with forests (84.1 – 88.5% resp.) and paddy fields (0.6 – 0.8 % resp.), other cropland (12.1 – 9.2 % resp.), urban areas (1.7 – 0.6% resp). This catchment drains the surfaces that received the highest levels of radiocesium ($^{134+137}Cs$) fallout in March 2011, although very heterogeneous radiocesium contamination levels are found across the catchment along the Ukedo and Takase rivers, where they range from 50 $kBq.kg^{-1}$ to 1800 $kBq.kg^{-1}$ (Fig. 1.) (JAXA, 2022; Kato and Onda, 2018). The upper part of these catchments is currently under decontamination, while the lower part has been fully decontaminated since March 2017 (Ministry of Environment, 2018).

2.2. Samples

The twenty-two samples investigated in the current research were collected in the downstream sections of the Ukedo (37.496692°N; 141.001488°E) and Takase (37.490175°N; 141.004735°E) rivers, just before their confluence (Fig. 1.). These lag deposit samples were comprised of fine particulate material that settled on channel banks, inset benches and floodplains during the falling limb of the last significant hydro-sedimentary event (Evrard et al., 2021). Sampling occurred bi-annually (i.e. in autumn after the typhoon season and in spring, after the snowmelt run-off) between May 2013 and November 2016. Then, the campaigns occurred only after the typhoon season late in October or early in November between 2017 and 2020 (Table S1) (Evrard et al., 2021). Samples were dried in an oven at 40 °C for 72 h, sieved to 2 mm, grounded to a fine powder using an agate mortar and stored at room temperature after preparation. This < 2 mm fraction was used for analysis.

2.3. Gamma spectrometry

Radionuclide activities (^{134}Cs, ^{137}Cs) in sediment samples were determined by gamma spectrometry using HPGe detectors. All samples (10 – 15 g of material depending on the density) were pressed into 15 mL polyethylene Petri dish containers for analysis. Counting time of sediment samples varied between 5 and 8 × 10^4 s, and activities were expressed in Bq per kg of dry weight ($Bq.kg^{-1}$) and decay-corrected to January 2021. Quality assurance was conducted using certified International Atomic Energy Agency (IAEA) reference materials (i.e. IAEA-444, IAEA-375) as well as a multi-gamma resin produced by the IRSN (Institut de Radioprotection et de Sûreté Nucléaire, France), with elevated ^{137}Cs (160 $kBq.kg^{-1}$; reference date: January 7, 2011) and ^{134}Cs activities (330 $kBq.kg^{-1}$) prepared in the same containers as the samples.

2.4. Samples chemical preparation and purification for plutonium analysis

Samples were divided into 4 analytical batches containing 5 to 8 samples and 3 analytical blanks. For each sample, ~ 5 g-aliquots were transferred in Pyrex® beakers covered with watch glasses and carbonized at 450 °C for 12 h in an electric furnace to decompose organic matter. After cooling, samples were transferred in 60 mL Savillex® beakers by adding HNO_3 (10 mL) and H_2O (5 mL, 3 times), and an evaporation to dryness was carried out. A first leaching on hot plate (150 °C) with HNO_3 (20 mL) and evaporation to dryness was performed. After cooling, a limited amount of ^{244}Pu (~ 100 fg) was added to the samples as isotopic dilution tracer for plutonium quantitative analysis. The ^{244}Pu tracer was used because this isotope was not found in the samples and therefore allows for plutonium quantification. The other steps of separation and purification of plutonium followed the method used by Jaegler et al. (2019, 2018).

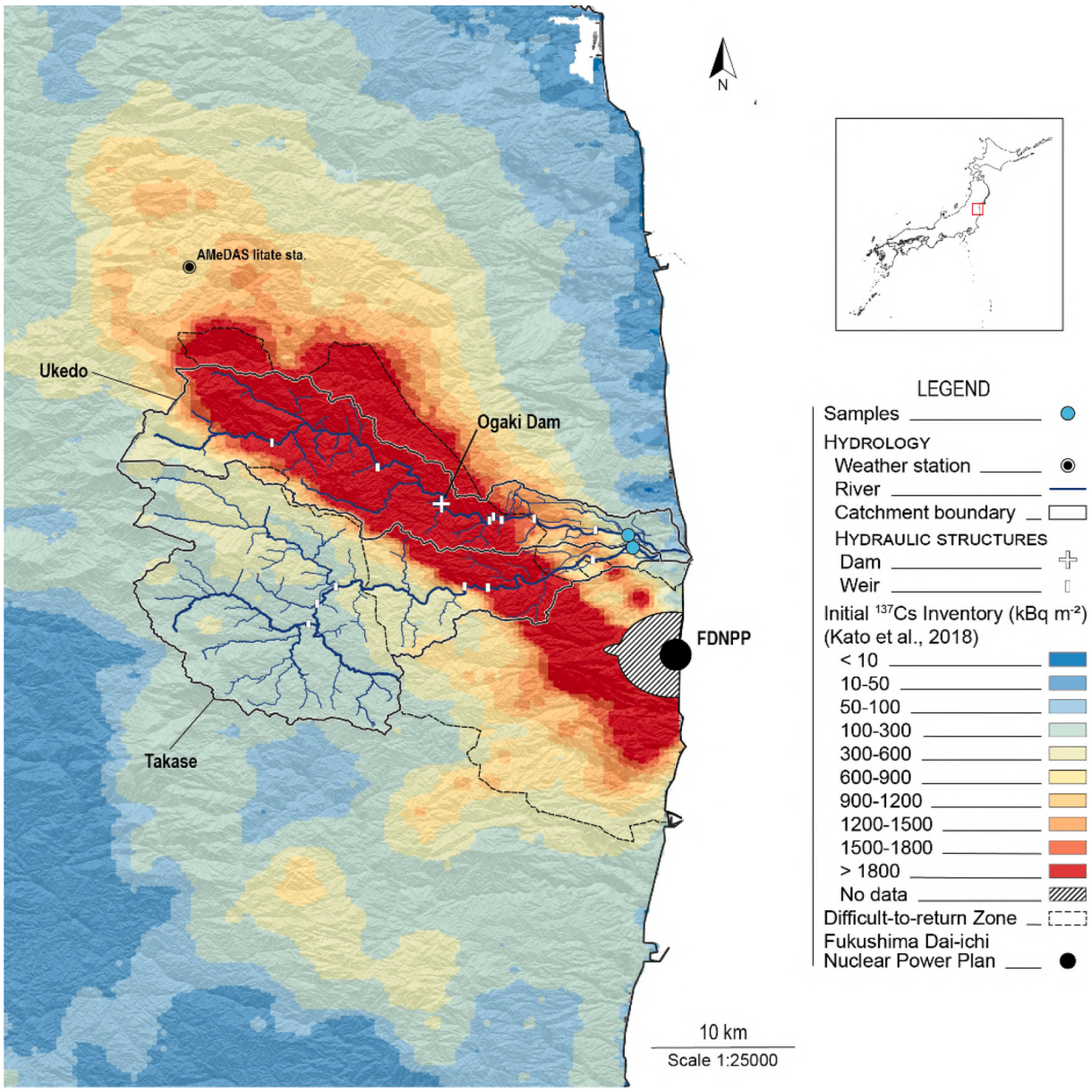

Fig. 1. Background ^{137}Cs level map in soils of the Fukushima Prefecture after Kato and Onda, (2018) with location of the Fukushima Dai-Ichi Nuclear Power Plant, the investigated river catchments, the location of the sediment lag deposit samples (blue dots), and the Difficult-To-Return Zone. (For interpretation of the references to colour in this figure legend, the reader is referred to the Web version of this article.)

2.5. ICP-MS measurements

Pu isotopic composition, activity concentration and concentrations were measured with a multi-collection ICP-MS ("Neptune Plus", Thermo-Fisher, Bremen, Germany). Instrumental settings used to perform the isotopic plutonium measurements were the same as those detailed by Jaegler et al. (2019, 2018). The measured isotopes are ^{239}Pu, ^{240}Pu, ^{241}Pu and ^{242}Pu. All plutonium activity concentrations and isotopic ratios presented in the current research were corrected by the average of analytical blanks for each batch. The validity of the analytical measurements and the correction method were verified by analysing the IAEA-385 certified material for the ^{240}Pu/^{239}Pu ratio. The certified value is 0.168 (± 0.016) and the measured value is 0.168 (± 0.011) with a confidence level of 95 % for each value. During the analyses, the blank values varied between 4.0 (± 0.8) fg and 12.1 (± 8.6) fg and the chemical efficiency between 26 % (± 3 %) and 100 % (± 2 %) (Detailed in Table S1).

2.6. Organic matter property measurements

Both total carbon and organic carbon fractions, from the bulk sediment were analysed in all samples. Approximately 15–20 mg of sediment was weighed in tin cups for analysis (with a precision of 1 µg). The sample was combusted in an elementary analyser (FlashEA1112, Thermo Fisher Scientific), and the carbon content determined using the Eager software. A standard was inserted every 10 samples. The inorganic carbon content in the bulk sediment was calculated by assuming that mineral carbon exists only as $CaCO_3$. The results are reported in % weight of carbonate/bulk sediment and in %weight of organic carbon/bulk sediment.

2.7. Carbon stable isotopic signatures

Analysis was performed online using a continuous flow EA-IRMS coupling, i.e. a FlashEA1112 Elemental Analyser coupled to a

ThermoFinigan Delta + XP Isotope-Ratio Mass Spectrometer. Three in-house standards (Hobo5 sediment - $\delta^{13}C = -13.4‰$, oxalic acid 2 - $\delta^{13}C = -16.7‰$, and GCL - $\delta^{13}C = -26.7‰$) were inserted every five samples. Each in-house standard was regularly checked against international standards. The results are reported in the δ notation: $\delta^{13}C = (R_{sample}/R_{standard} - 1)$, where R_{sample} and $R_{standard}$ are the $^{13}C/^{12}C$ ratios of the sample and the international standard, Vienna Pee Dee Bee (VPDB), respectively.

2.8. Particle size analyses

Particle size analyses were performed on all sediment samples by laser granulometry (Mastersizer® 3000, 194 Malvern Instruments, Ltd., UK) This technology provides the advantage of providing data on the particle size distribution between 0.01 and 3500 μm and the corresponding particle size distribution at 10 % (D10), the median particle size (D50), and that at 90 % (D90). The Specific Surface Area (SSA) was also determined during the analysis assuming that the particles are spherical.

2.9. Statistical treatment

In order to better understand the distribution and control factors of Pu in each river, correlations with other radionuclide concentrations and sediment properties were assessed. The Pearson (linear) and Spearman (non-linear) correlations were calculated using the *cor* function from *stats* package (R Core Team, 2021). Significance of correlations was assessed using the *cor. mtest* function from *corrplot* package (Wei and Simko, 2021) for each type of correlation. Only correlations with a significance test p-value below $\alpha = 0.05$ were considered as significant and were retained. When both linear and non-linear correlations were significant, only the correlation with the highest value was retained. Correlations with an absolute value above 0.50 were represented with a correlogram.

3. Results and discussion

3.1. Changes in Pu activity concentrations in river sediment from 2013 to 2020

Pu activity concentrations were found to vary from 0.031 to 0.758 $mBq.g^{-1}$ in the Ukedo River sediment and from 0.015 to 0.138 $mBq.g^{-1}$ in the Takase River sediment (Table 1). Globally, the plutonium activity concentrations were higher in the Ukedo River (mean value: 0.173 $mBq.g^{-1}$) than in the Takase River (mean value: 0.049 $mBq.g^{-1}$). However, a global decrease in concentrations was observed with time with some sporadic increases induced by typhoons. Several studies have quantified the Pu activity concentrations in different environments, all along the entire continent-to-ocean continuum (Fig. 2).

Previous studies indicate a strong decreasing activity concentration gradient from the upstream sources in the soils to the marine sediment where contaminated material deposits (Bu et al., 2015b; Cao et al.,

Table 1
Plutonium activity concentrations and $^{240}Pu/^{239}Pu$ isotopic ratios measured in lag deposit samples collected in the Ukedo River and Takaser River from 2013 to 2020. The grey cell corresponds to the value obtained on a sample already analysed by a previous study. All uncertainties are combined expanded uncertainties with a confidence level of 95 %.

Sample ID	Sampling date	Location	$^{240}Pu/^{239}Pu$ isotopic ratio	$^{239+240}Pu$ activity concentration ($mBq.g^{-1}$)
FEL_383	09/05/2013	Ukedo	0.182 ± 0.010	0.229
FEL_385	09/05/2013		0.172 ± 0.012	0.758
FEL385 Evrard et al. (2014)	09/05/2013		0.181 ± 0.006	0.827
FEL_519	02/11/2013		0.175 ± 0.014	0.353
FEL_616	10/05/2014		0.179 ± 0.024	0.066
FEL_648	30/10/2014		0.187 ± 0.017	0.114
FEL_762	26/03/2015		0.187 ± 0.013	0.144
FEL_932	05/11/2015		0.206 ± 0.031	0.025
FEL_1004	23/06/2016		0.181 ± 0.012	0.119
FEL_1043	02/11/2016		0.186 ± 0.041	0.031
FEL_1322	25/10/2017		0.174 ± 0.009	0.087
FEL_1416	31/10/2018		0.186 ± 0.013	0.104
FEL_1521	30/10/2020		0.197 ± 0.054	0.045
FEL_615	05/10/2014	Takase	0.168 ± 0.031	0.033
FEL_647	30/10/2014		0.196 ± 0.035	0.034
FEL_761	26/03/2015		0.187 ± 0.032	0.031
FEL_931	05/11/2015		0.183 ± 0.019	0.138
FEL_1003	23/06/2016		0.171 ± 0.015	0.115
FEL_1042	02/11/2016		0.194 ± 0.020	0.030
FEL_1321	25/10/2017		0.182 ± 0.022	0.025
FEL_1417	31/10/2018		0.193 ± 0.051	0.024
FEL_1522	30/10/2020		0.220 ± 0.047	0.015

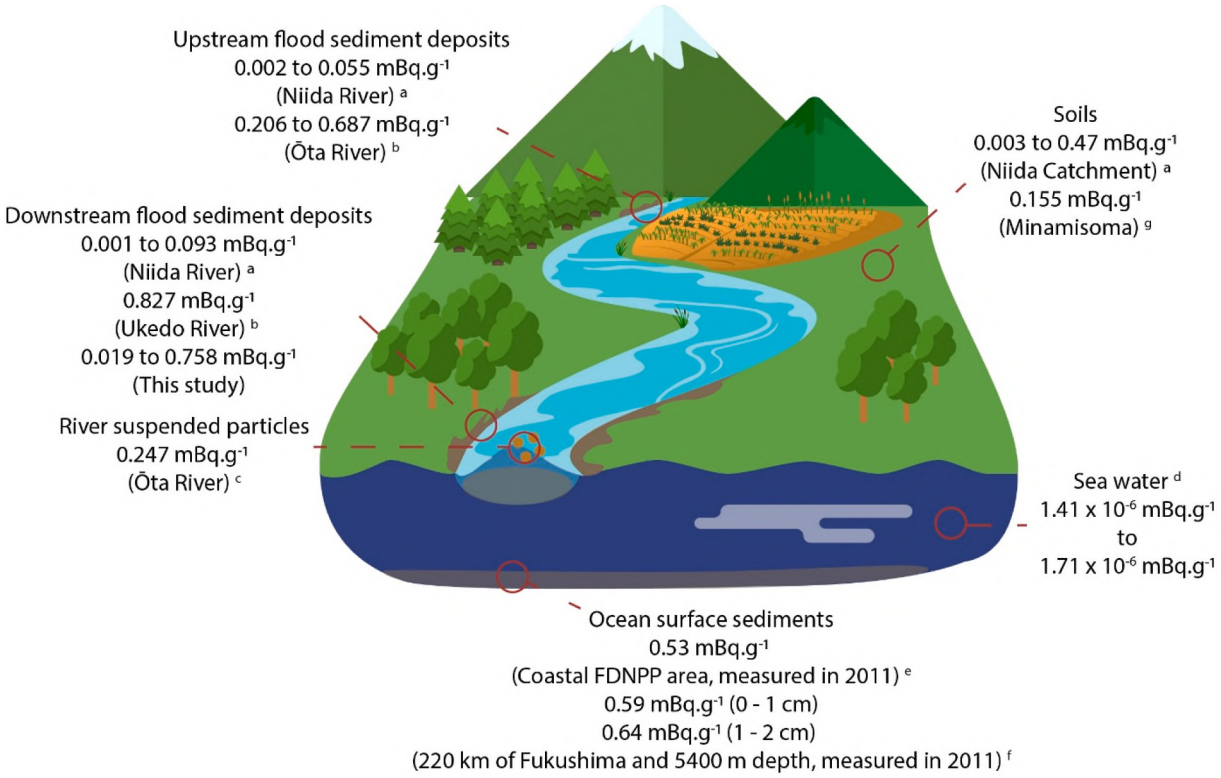

Fig. 2. Sketch illustrating the Pu activity concentration variations (all values were decay-corrected to March 2021) along the continent-to-ocean continuum. **a** (Jaegler et al., 2018).; **b** (Evrard et al., 2014).; **c** (Cao et al., 2016).; **d** (Men et al., 2018).; **e** (Oikawa et al., 2015).; **f** (Bu et al., 2015b).; **g.** (Schneider et al., 2013).

2016; Evrard et al., 2014; Jaegler et al., 2018; Men et al., 2018; Oikawa et al., 2015; Schneider et al., 2013). On the continent (soils and flood sediment deposits), activity concentrations up to ~1.5 millibecquerel per gram (from 1.56 to 0.015 mBq.g^{-1}) were measured with a global decrease over time (0.007 mBq.g^{-1} in 2011 in Niida sediment to 0.001 mBq.g^{-1} in 2020 in Takase sediment). In contrast, the lowest activity concentrations, in the nanobecquerel per gram range ((1.41 – 1.71) x 10^{-6} mBq.g^{-1}), were obtained in seawater. Ocean surface sediment show intermediate activity concentrations between 0.53 mBq.g^{-1} and 0.64 mBq.g^{-1}. Lower plutonium activity concentrations are observed in the marine environment, probably due to the dilution of particles induced by the strong Kuroshio current (Buesseler et al., 2015; Men et al., 2018). In these studies, a similar decrease and dilution effect of ^{137}Cs from the Ukedo River and Takase River was observed in the marine environment, and it was found that the total contribution of the ^{137}Cs from these rivers represented only 7 % of the total annual inventory supplied to seabed sediments (Misonou et al., 2022). Therefore, it is expected that a similar contribution of plutonium may be supplied by these rivers to marine environments but its source is not necessarily identical to that of cesium one because a strong contribution from global fallout is observed.

3.2. *Changes in plutonium isotopic signatures in river sediment*

In this study, we focused the interpretation on the ^{240}Pu/^{239}Pu isotopic ratio, because ^{241}Pu and ^{242}Pu are below the detection limits (concentrations presented in Table S2). This represents a major change compared to earlier publications (Evrard et al., 2014; Jaegler et al., 2018) that detected ^{241}Pu and demonstrated thereby a significant supply of Pu from the FDNPP accident. Similarly as for ^{241}Pu, ^{242}Pu is not used for the interpretation in the current research, as this isotope was systematically found below the analytical detection limits (around 0.1 fg for Pu isotopes) whereas it had been detected by Jaegler et al. (2018). The Ukedo lag deposit referred to as FEL385 sampled in May 2013 was also analysed by Evrard et al. (2014) and the value found in the current research (0.181 (± 0.006)) remains very close and not significantly different from that found in 2014 (0.172 (± 0.012)). In the current research, the ^{240}Pu/^{239}Pu isotopic ratios were measured for all Ukedo and Takase flood sediment deposit samples. Results are provided in Table 1, and the temporal evolution of this isotopic ratio is shown in Fig. 3A For the Ukedo River and in Fig. 3B For the Takase River.

The ^{240}Pu/^{239}Pu isotopic ratio and its changes with time provide information on the origin and fate of plutonium found in the Ukedo and Takase rivers. The ^{240}Pu/^{239}Pu isotopic ratio values may be compared to those of global fallout in the northern hemisphere as determined by Kelley et al. (1999) (0.180 (± 0.014)), and to the signatures of the FDNPP reactors estimated by the model simulations conducted by Nishihara et al. (2012) (reactor 1 : 0.339; reactor 2 : 0.315; reactor 3 : 0.351) (Fig. 3). For the Ukedo lag deposits, the ^{240}Pu/^{239}Pu isotopic ratio ranged between 0.172 (± 0.012) and 0.206 (± 0.031) (see Fig. 3A). For the Takase lag deposits, the ^{240}Pu/^{239}Pu isotopic ratio ranged between 0.168 (± 0.031) and 0.220 (± 0.047) (see Fig. 3B).

^{240}Pu/^{239}Pu isotopic ratios measured in this study are not significantly different from those associated with the global fallout. Values of this isotopic ratio in Japanese soils, sediments and lag deposits were reported in several publications (Evrard et al., 2014; Jaegler et al., 2019, 2018; Schneider et al., 2017; Steinhauser et al., 2015; Yang et al., 2017; Zheng et al., 2013, 2012), and, for those samples collected until 2013, some of the measured values were much closer to the Fukushima Pu source signature (Evrard et al., 2014; Jaegler et al., 2019; Schneider et al., 2017; Yang et al., 2017). Yang et al. (2017) analysed the ^{240}Pu/^{239}Pu isotopic ratio in soils sampled in 2011 in the Fukushima Prefecture with values ranging between 0.245 (± 0.014) and 0.312 (± 0.044). Evrard et al. (2014) collected lag deposits from Niida, Ota and Ukedo Rivers between November 2011 and May 2013, and obtained ^{240}Pu/^{239}Pu isotopic ratios between 0.150 (± 0.005) and 0.281 (± 0.012). Jaegler et al. (2019) analysed soil samples collected between November 2011 and November 2012 in the Mano River catchment

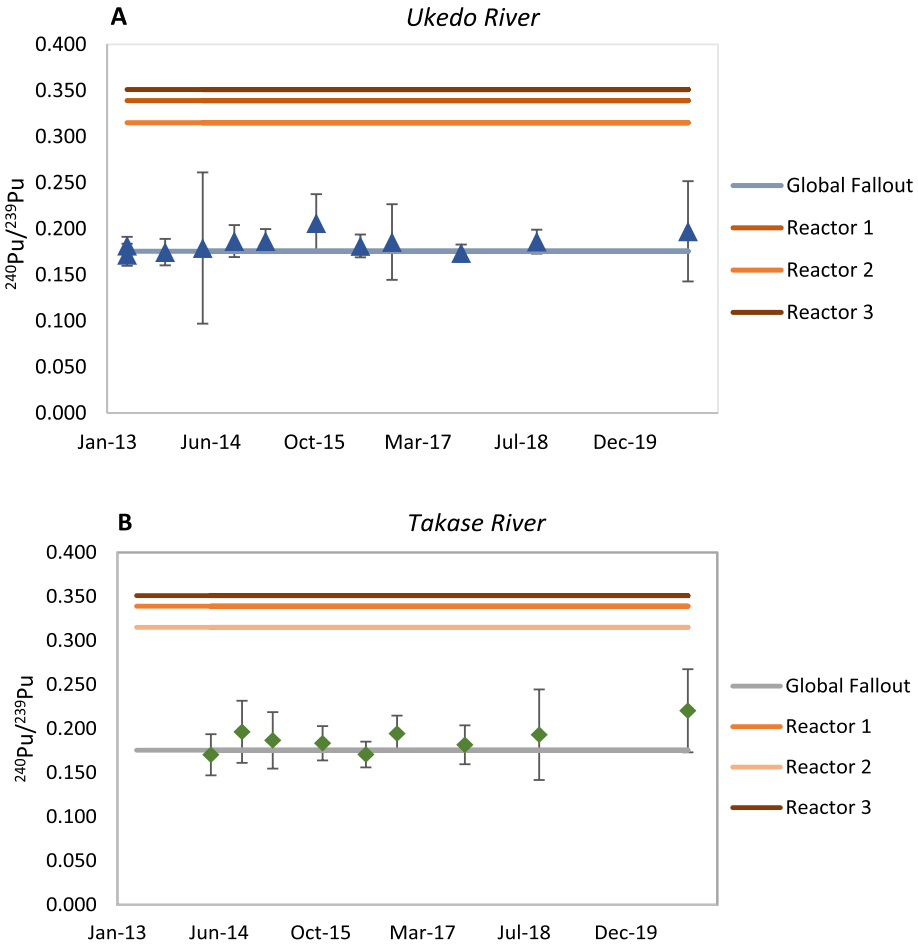

Fig. 3. Evolution of $^{240}Pu/^{239}Pu$ isotopic ratios between 2013 and 2020 in the (A) Ukedo River sediment and (B) the Takase River sediment. The grey line corresponds to the mean of the global fallout signature in the northern hemisphere (Kelley et al., 1999). The orange lines correspond to the estimated source values of the FDNPP reactors (Nishihara et al., 2012). All uncertainties are combined expanded uncertainties with a confidence level of 95 %. (For interpretation of the references to colour in this figure legend, the reader is referred to the Web version of this article.)

located further to the North from FDNPP compared to the Ukedo River catchment. $^{240}Pu/^{239}Pu$ isotopic ratios values in these samples ranged between 0.177 (± 0.014) and 0.285 (± 0.049). This isotopic ratio was also investigated by Steinhauser et al. (2015) in soil samples collected in Minami-soma on September 7, 2014, and values ranged between 0.160 and 0.220 (Fig. S3). Then, in contrast, values obtained on environmental samples collected after 2013 remained in the range of signatures attributed to the global fallout. In the current research, these values ranged between 0.168 (± 0.031) and 0.220 (± 0.047). Schneider et al. (2017) studied soil samples from Minami-soma City and Okuma Town collected in June 2013 and May 2015.$^{240}Pu/^{239}Pu$ isotopic ratios ranged between 0.18 and 0.48 (± 0.15) in 2013, whereas the samples taken is 2015 showed rather constant values close to 0.18. Overall, the current results show that (1) the global fallout provides the main source of Pu to sediment whatever the sampling year after FDNPP accident, and (2) the currently negligible contribution of the FDNPP accident of Pu to the sediment. Accordingly, the current research provides a useful complement to the conclusions made by Jaegler et al. (2018) who estimated very low FDNPP contributions (ranging between 1.2 % (± 1.4 %) and 10.4 % (± 3.1 %)) to plutonium supply in sediment of the Niida River.

3.3. *Evolution of sediment properties from 2013 to 2020*

The temporal evolution of rainfall and some sediment properties such as ^{137}Cs activity concentrations, median particle size (D50), SSA, C/N ratios and $\delta^{13}C$ values was considered in order to improve our understanding of the radionuclide control factors in sediment (All the data are available online: https://doi.org/10.5281/zenodo.7233904 (Diacre et al., 2022)). Sediment properties are provided in Fig. 4, and their temporal evolution is shown in Fig. 4A for the Ukedo River, and in Fig. 4B for the Takase River. Pu concentrations and the $^{239+240}Pu/^{137}Cs$ ratio are available in Table S4.

First, the ^{137}Cs activities show a global decrease and different patterns of temporal variations between the two rivers. In the case of the Ukedo River, ^{137}Cs activities ranged between 2.5 $kBq.kg^{-1}$ and 83.2 $kBq.kg^{-1}$, with the highest ^{137}Cs activities recorded in Spring in 2013 (Fig. 4A.). The evolution of the ^{137}Cs activity in lag deposits collected at this location was not impacted by the occurrence of heavy rainfall events (typhoons and tropical storms). In contrast, the ^{137}Cs activities measured in the Takase River were lower than those found in the Ukedo River sediment, as they ranged between 0.1 $kBq.kg^{-1}$ and 27.5 $kBq.kg^{-1}$ (Fig. 4B.), with the highest value observed after Typhoon Etau in 2015. The difference in ^{137}Cs activity levels and variations between both rivers may be related to (1) the different levels of initial contamination in their respective drainage areas, as observed in Fig. 1, and (2) a difference in decontamination phases in the watershed, which may control inputs especially during strong variations (Feng et al., 2022; Onda et al., 2020). The absence of correlation between rainfall depths and ^{137}Cs activities in sediment in the Ukedo River is likely related to the presence of Ogaki Dam 18 km upstream of the sampling location (Yamada et al., 2015). It was estimated that only 10% of the sediment transported by the Ukedo River upstream of Ogaki Dam reaches the river outlet (Kitamura et al., 2014). However, according to the literature, the overall decrease in ^{137}Cs shows a similar trend upstream and downstream of the dam (Feng et al., 2022). For both Ukedo and Takase Rivers, the ^{137}Cs activity evolution shows the same trend as for the Pu concentration (Fig. 4).

Then, granulometric parameters were also considered to characterize the sediment properties carrying the radionuclides of interest. In

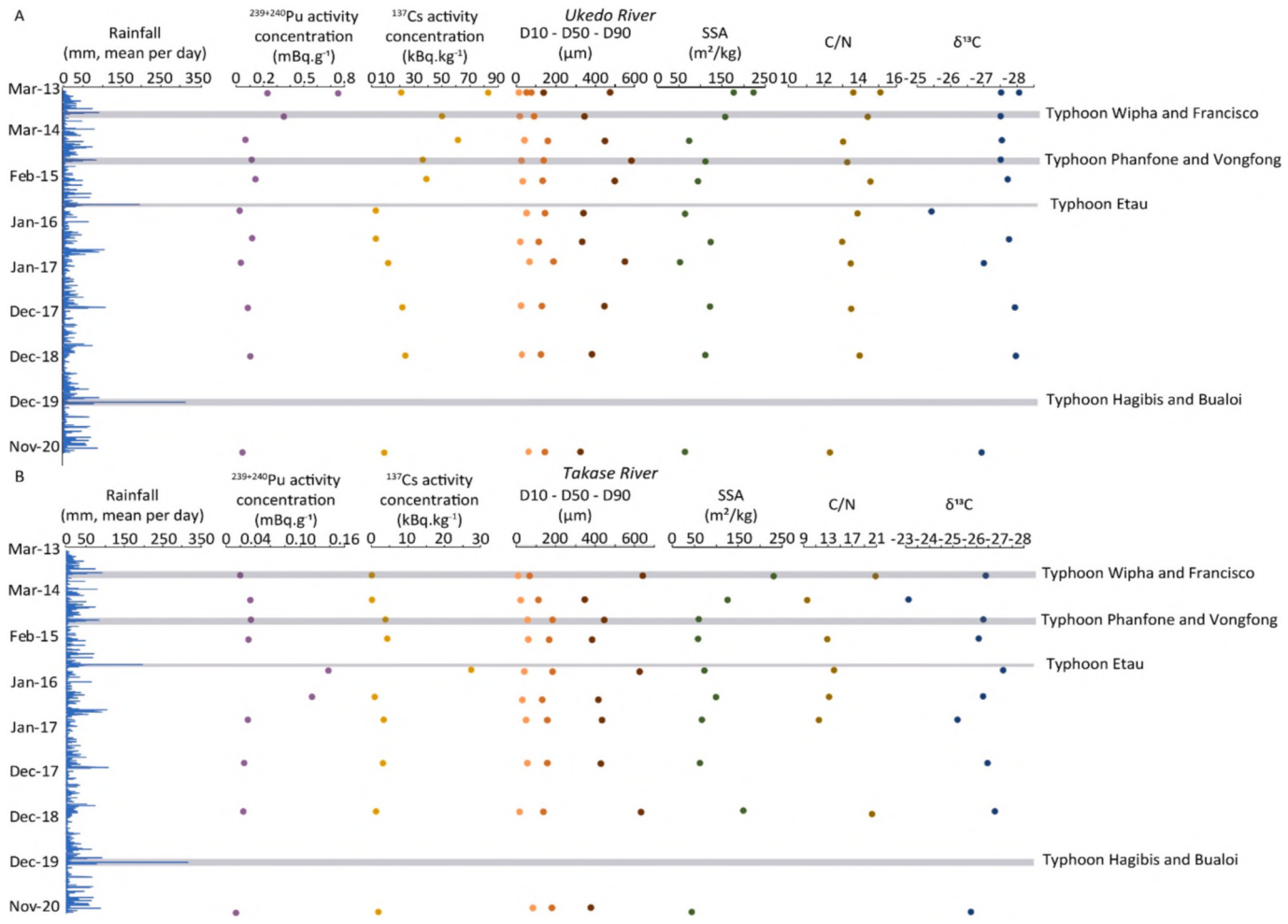

Fig. 4. $^{239+240}$Pu and^{137}Cs activity concentrations, D10 - D50 – D90, SSA, C/N and δ^{13}C analysed in this study. **A.** Results for the Ukedo River sediment, and **B.** for the Takase River sediment. Main typhoons that occurred during this period are reported (Evrard et al., 2020; Laceby et al., 2016a). The mean daily rainfall is plotted for the station Iitate (37.665 N, 140.727 E) (Japanese Metereological Agency, 2021).

both rivers, the same inter-event variations of the D50 were observed, and similar mean particle size values of 126 µm and 146 µm were found for both Ukedo and Takase Rivers, respectively (Fig. 4). These mean D50 values show that the flood deposit sediments are mainly composed of fine sands, although the Ukedo River sediment contained a higher proportion of fine minerals (i.e. silt and clay minerals) (Fig. S5). Logically, a similar interpretation can be made for the SSA parameter, with mean values of 115 and 98 m^2/kg for the Ukedo River and Takase River, respectively (Fig. 4). An anti-correlation was observed between the D50 and the SSA, with the latter being correlated to the finest particles, which likely explains why the lowest value of this parameter was recorded during the heaviest rainfall events until 2015. Typhoon Etau in 2015 likely flushed most of the contaminated material stored in the river channels or in their close vicinity since 2011 as demonstrated in previous research (e.g. Chartin et al. (2017); Evrard et al. (2021)).

Finally, the δ^{13}C and the C/N parameters allowed identifying the main source of the organic matter of sediment transiting both rivers. A δ^{13}C difference is observed between the Ukedo and Takase rivers although their catchment drainage areas have similar land use distributions, which likely indicates that different sediment sources were mobilized in both catchments (Nakanishi et al., 2021). The entire δ^{13}C value ranges observed over the period 2013–2020 are comprised between −25.42 ‰ and −28.07 ‰ for the Ukedo River, compared to an interval comprised between −23.10 ‰ and −27.11 ‰ for the Takase River (Fig. 4). These δ^{13}C values show that the organic matter found in sediment mainly originates from terrestrial plants and particularly from C_3 plants (Lamb et al., 2006). Based on sediment source data from neighbouring catchments, material fluxes from the Ukedo River are therefore mainly supplied by soils under forest (δ^{13}C values ranging between −28 and −26 ‰), while those from Takase River are likely mainly delivered by cultivated soils or subsoils (δ^{13}C values ranging between −26.5 and −22‰) (Laceby et al., 2016b). This diagnosis is further supported by the analysis of C/N ratios for both the Ukedo and Takase river sediment, with mean respective values of 13.4 and 13.7 (Fig. 4). The mean value is representative of that of the only source for the Ukedo River, while for the Takase River values ranged between 9.5 and 20.8, which is likely indicative of the occurrence of two main sediment sources (cultivated soils and subsoils). The C/N values exceeding 12 correspond to organic matter of plants composed of lignin and cellulose, as cedar, pine, and oak characteristic of forest soils (Lamb et al., 2006). This source clearly dominated the contributions of the Ukedo River organic matter inputs, while it partly contributed to those of the Takase River. In the latter, the rest of the material was supplied by sources with C/N values ranging between 10 and 12 and corresponding to vascular plant sources, as cultivated plants, as observed in the Takase River sediment collected in May 2014 and November 2016. The interpretations made based on C/N values are in agreement with those made based on δ^{13}C values.

3.4. Statistical approach to determine the control factors of the Pu concentration evolution

In the previous section, we observed that Pu concentration variations tend to follow those of Cs although their emission origins are distinct. This demonstrates the same mode of transport of radionuclides regardless of their source. Their input to the outlet is therefore mainly controlled by fluctuations in precipitation, runoff, erosion. To complement this finding and derive further information about the behaviour of these radionuclides, a statistical approach plotting the Pearson correlation coefficients calculated between radionuclide concentrations and other sediment properties was conducted under the form of a heatmap.

The results show that the two investigated rivers show differences in the dynamics of Pu transportation as inferred from the correlations between the tested parameters (Fig. 5).

In the case of the Ukedo River, Pu concentrations showed significant and high positive linear correlations with ^{137}Cs and ^{134}Cs activities (r of 0.75 and 0.76 resp.) and C/N ratio (r of 0.72). Furthermore, the analysis showed high non-linear correlations with sediment properties with, on the one hand, anti-correlations with grain size parameters (D10: r = -0.87; D50: r = - 0.87) and, on the other hand, positive correlations with SSA (r = 0.87) and with organic matter parameters (C: r = 0.97; N: r = 0.95) (Fig. 5A). These results suggest that Pu was transported in association with organic matter or fine minerals (high anti-correlation with D10 and D50), while the high correlation with SSA suggests its strong affinity for clay materials, as it was demonstrated for ^{137}Cs (Feng et al., 2022; Hirose, 2022; Onda et al., 2020). Other radionuclides (i.e. ^{137}Cs and ^{134}Cs), showed the same trend in their correlations, although only linear correlations were observed with them. Based on the literature, ^{137}Cs is mainly sorbed onto the surface of minerals (i.e. mainly clays minerals), and its transport also shows some level of land use dependency (Feng et al., 2022; Hirose, 2022; Onda et al., 2020). The non-linear relationship of Pu with grain size and organic matter, in contrast to ^{137}Cs and ^{134}Cs, suggests another way of transport in addition to sorption. According to the literature, the $^{239+240}$Pu activity concentration increases in the lowest particle size fractions as for ^{137}Cs. However, in contrast to ^{137}Cs, $^{239+240}$Pu is known to be associated not only with clays but also with organic matter and oxides (for example through organic and inorganic colloids). Furthermore, their stability in solution increases when they are multiphase (organic + inorganic) (Alewell et al., 2017; Kersting, 2013; Romanenko and Lujanienė, 2022; Xu et al., 2017). Finally, Romanenko and Lujanienė (2022) showed that Pu(IV) reacts actively with colloids and suspended solids while Pu(V) reacts with carbonate particles. In the case of this study, Pu was likely under the form Pu(IV) since it is associated with fine particles (clays, silts, organic matter). The presence of the Ogaki dam upstream (Kitamura et al., 2014) may impact Pu transport. Therefore, the transport of material downstream is likely controlled by the outflow discharge from the dam with only 10 % of the inflow being transferred downstream (Nakanishi et al., 2021). Moreover, as it was shown that sands are deposited preferentially upstream of Ogaki Dam, silt deposits would occur across the reservoir and clays would remain in suspension, deposit nearby the dam and part of this fine material may eventually be transferred to the downstream river section where the samples analysed in the current research were collected, which highlights the major role of the dam (Yamada et al., 2015).

Similarly, Pu concentrations in the Takase River sediment were found to be highly linearly correlated to ^{137}Cs and ^{134}Cs activities (Fig. 5B) (r = 0.69). However, in contrast with what was observed for the Ukedo River, no sediment property was found to be correlated with Pu concentrations. In addition, ^{137}Cs and ^{134}Cs activities were showed to be non-linearly correlated with sediment properties while they were linearly correlated with these properties in the Ukedo River.

Although these two rivers are geographically very close, they showed different sediment dynamics and characteristics. Overall, the Ukedo River flood deposit sediment contained finer particles (silts, clays, fine sands) than in the Takase River (Fig. S5). These different properties with coarser particles transiting in the Takase River compared to the Ukedo River are likely related to the presence of Ogaki Dam along the latter, leading to a preferential transport of the finest fractions from upper to lower catchment parts. In contrast, the flow of the Takase River is not regulated and the river drains less contaminated soils (± 47% of the catchment surface), which likely explains why the statistical analysis led to less clear results for Pu in this second river.

4. Conclusions

In the current research, Pu concentrations were measured in flood

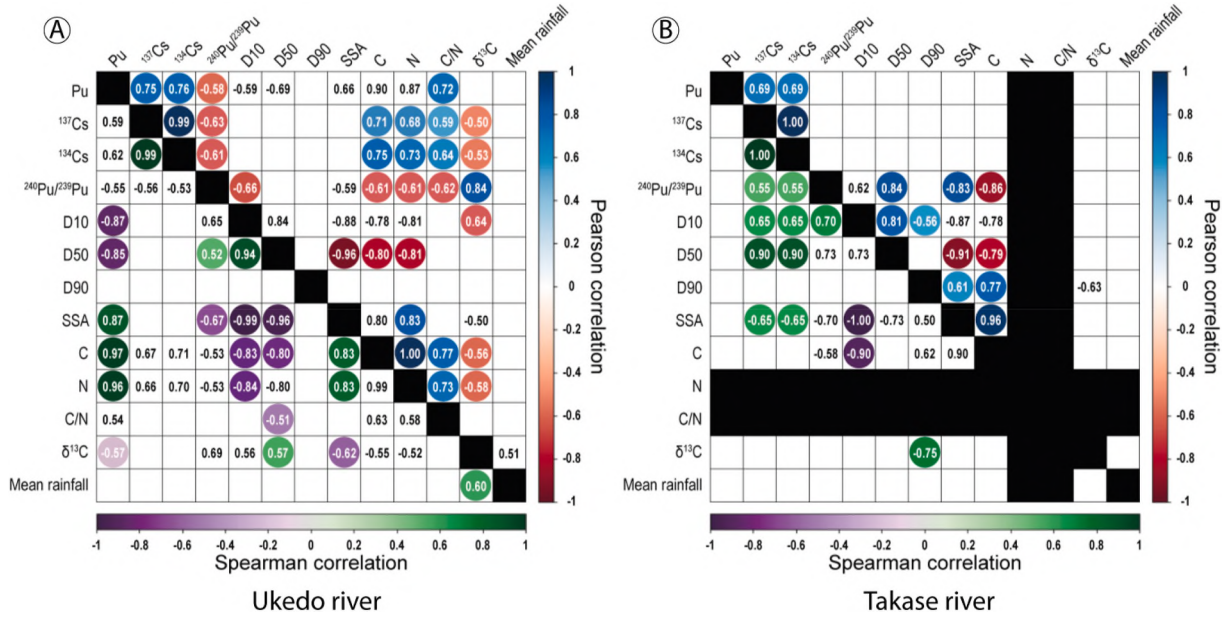

Fig. 5. Significant Pearson (linear; upper part) and Spearman (non-linear; lower part) correlation matrices between radionuclide and sediment properties above 0.5, for (**A**) Ukedo river (n = 12) and (**B**) Takase river (n = 10). The highest correlation and anti-correlation values between both modes (i.e., linear and non-linear) are indicated with a coloured circle.

deposit sediments collected in lower sections of the Ukedo and the Takase rivers from 2013 to 2020. For both Ukedo and Takase rivers, a global decrease in Pu concentrations (following that of ^{137}Cs activity concentrations) was observed throughout time possibly in response to the abandonment of the region after the accident and the progressive exhaustion of the easily mobilized contaminated particles stored in the main river channels and in their vicinity after 2011 and until typhoon Etau in 2015. This situation allowed vegetation to re-grow, which protected the contaminated soils from surface erosion, and subsurface erosion mobilized instead the deeper soil layers that were not contaminated by the FDNPP accident or forest soils that are mainly found on steeper slopes in the case of the Ukedo River. In addition to the quantification of Pu concentrations, the determination of Pu isotopic ratios provided additional information on this actinide source. Contrary to studies conducted early after the FDNPP accident on environmental samples collected until 2013, in the current research, flood deposit sediments showed a ^{240}Pu/^{239}Pu signature (ranging between 0.168 and 0.220) coinciding with that of the global fallout (around 0.180 in the Northern hemisphere). Accordingly, in sediment collected between 2013 and 2020, the impact of the FDNPP fallout on sediment contamination with Pu had become negligible despite the occurrence of multiple heavy rainfall events in the region during this period and the fact that these rivers are located in the vicinity of FDNPP and drain a significant part of the Difficult-to-Return Zone. Differences of the hydro-sedimentary properties found in both rivers was also highlighted, probably induced by the presence of the Ogaki dam on the Ukedo River, that highly impacted the radionuclide transfer from the Difficult-to-Return zone to the Pacific Ocean.

Currently, decontamination work is underway in the area, and it would be interesting to investigate variations in ^{137}Cs activities, Pu concentrations and sediment sources during this major land cover change process. Indeed, a similar study could be conducted across the area after its reopening in 2023, in order to detect potential changes, including those related to a potential Pu remobilization, after remediation that may expose contaminated soil layers that were protected by vegetation regrowth after land abandonment until the recent decontamination works.

Author statement

Aurélie Diacre: Writing – original draft, Investigation, Formal analysis, Data curation. Thomas Chalaux Clergue: Writing – original draft, Data curation. Soazig Burban: Formal analysis. Caroline Gauthier: Formal analysis, Amélie Hubert: Data curation. Anne-Claire Humbert: Resources. Irène Lefevre: Formal analysis, Data curation. Anne-Laure Fauré: Supervision. Fabien Pointurier: Review – Supervision. Olivier Evrard: Writing - Review, Supervision, Resources, Sampling, Fieldwork.

Declaration of competing interest

The authors declare that they have no known competing financial interests or personal relationships that could have appeared to influence the work reported in this paper.

Data availability

Data are available online: https://doi.org/10.5281/zenodo.7233904

Acknowledgements

Aurélie Diacre received a PhD fellowship from CEA (Commissariat à l'Energie Atomique et aux Energies Alternatives, France). Sample collection was supported by MITATE Lab (CNRS International Research Project) and AMORAD projects (Programme d'Investissements d'Avenir en Radioprotection et Sûreté Nucléaire, grant no. ANR-11-RSNR-0002). The authors are also grateful to Dr. Christine Hatté (GEOTRAC, LSCE) for the organic matter analyses.

Appendix A. Supplementary data

Supplementary data to this article can be found online at https://doi.org/10.1016/j.envpol.2022.120963.

References

Adachi, K., Kajino, M., Zaizen, Y., Igarashi, Y., 2013. Emission of spherical cesium-bearing particles from an early stage of the Fukushima nuclear accident. Sci. Rep. 3, 2554. https://doi.org/10.1038/srep02554.

Alewell, C., Pitois, A., Meusburger, K., Ketterer, M., Mabit, L., 2017. 239+240Pu from "contaminant" to soil erosion tracer: where do we stand? Earth Sci. Rev. 172, 107–123. https://doi.org/10.1016/j.earscirev.2017.07.009.

Aliyu, A.S., Evangeliou, N., Mousseau, T.A., Wu, J., Ramli, A.T., 2015. An overview of current knowledge concerning the health and environmental consequences of the Fukushima Daiichi Nuclear Power Plant (FDNPP) accident. Environ. Int. 85, 213–228. https://doi.org/10.1016/j.envint.2015.09.020.

Bu, W., Ni, Y., Guo, Q., Zheng, J., Uchida, S., 2015a. Pu isotopes in soils collected downwind from Lop Nor: regional fallout vs. global fallout. Sci. Rep. 5, 12262 https://doi.org/10.1038/srep12262.

Bu, W., Zheng, J., Guo, Q., Aono, T., Otosaka, S., Tagami, K., Uchida, S., 2015b. Temporal distribution of plutonium isotopes in marine sediments off Fukushima after the Fukushima dai-ichi nuclear power plant accident. J. Radioanal. Nucl. Chem. 303, 1151–1154. https://doi.org/10.1007/s10967-014-3437-y.

Buesseler, K.O., German, C.R., Honda, M.C., Otosaka, S., Black, E.E., Kawakami, H., Manganini, S.J., Pike, S.M., 2015. Tracking the fate of particle associated Fukushima daiichi cesium in the ocean off Japan. Environ. Sci. Technol. 49, 9807–9816. https://doi.org/10.1021/acs.est.5b02635.

Cao, L., Zheng, J., Tsukada, H., Pan, S., Wang, Z., Tagami, K., Uchida, S., 2016. Simultaneous determination of radiocesium (135Cs, 137Cs) and plutonium (239Pu, 240Pu) isotopes in river suspended particles by ICP-MS/MS and SF-ICP-MS. Talanta 159, 55–63. https://doi.org/10.1016/j.talanta.2016.06.008.

Chartin, C., Evrard, O., Laceby, J.P., Onda, Y., Ottlé, C., Lefèvre, I., Cerdan, O., 2017. The impact of typhoons on sediment connectivity: lessons learnt from contaminated coastal catchments of the Fukushima Prefecture (Japan): typhoon Impact on Sediment Connectivity - Fukushima, Japan. Earth Surf. Process. Landforms 42, 306–317. https://doi.org/10.1002/esp.4056.

Danesi, P.R., Moreno, J., Makarewicz, M., Louvat, D., 2008. Residual radionuclide concentrations and estimated radiation doses at the former French nuclear weapons test sites in Algeria. Appl. Radiat. Isot. 66, 1671–1674. https://doi.org/10.1016/j.apradiso.2007.08.022.

Diacre, A., Chalaux, T.G., Burban, S., Gauthier, C., Hubert, A., Humbert, A.-C., Lefevre, I., Evrard, O., 2022. Temporal Evolution of Plutonium Concentrations and Isotopic Ratios, Cesium Activity Concentrations, Granulometric Parameters and Organic Matter Properties in the Ukedo–Takase Rivers Draining the Difficult-To-Return Zone in Fukushima, Japan (2013–2020). https://doi.org/10.5281/zenodo.7233904.

Evrard, O., Chartin, C., Laceby, J.P., Onda, Y., Wakiyama, Y., Nakao, A., Cerdan, O., Lepage, H., Jaegler, H., Vandromme, R., Lefèvre, I., Bonté, P., 2021. Radionuclide contamination in flood sediment deposits in the coastal rivers draining the main radioactive pollution plume of Fukushima Prefecture, Japan (2011–2020). Earth Syst. Sci. Data 13, 2555–2560. https://doi.org/10.5194/essd-13-2555-2021.

Evrard, O., Chartin, C., Onda, Y., Patin, J., Lepage, H., Lefèvre, I., Ayrault, S., Ottlé, C., Bonté, P., 2013. Evolution of radioactive dose rates in fresh sediment deposits along coastal rivers draining Fukushima contamination plume. Sci. Rep. 3, 3079. https://doi.org/10.1038/srep03079.

Evrard, O., Durand, R., Nakao, A., Patrick Laceby, J., Lefèvre, I., Wakiyama, Y., Hayashi, S., Asanuma-Brice, C., Cerdan, O., 2020. Impact of the 2019 typhoons on sediment source contributions and radiocesium concentrations in rivers draining the Fukushima radioactive plume, Japan. Compt. Rendus Geosci. 352, 199–211. https://doi.org/10.5802/crgeos.42.

Evrard, O., Laceby, J.P., Lepage, H., Onda, Y., Cerdan, O., Ayrault, S., 2015. Radiocesium transfer from hillslopes to the Pacific Ocean after the Fukushima nuclear power plant accident: a review. J. Environ. Radioact. 148, 92–110. https://doi.org/10.1016/j.jenvrad.2015.06.018.

Evrard, O., Pointurier, F., Onda, Y., Chartin, C., Hubert, A., Lepage, H., Pottin, A.-C., Lefèvre, I., Bonté, P., Laceby, J.P., Ayrault, S., 2014. Novel insights into Fukushima nuclear accident from isotopic evidence of plutonium spread along coastal rivers. Environ. Sci. Technol. 48, 9334–9340. https://doi.org/10.1021/es501890n.

Feng, B., Onda, Y., Wakiyama, Y., Taniguchi, K., Hashimoto, A., Zhang, Y., 2022. Persistent impact of Fukushima decontamination on soil erosion and suspended sediment. Nat. Sustain. 1–11. https://doi.org/10.1038/s41893-022-00924-6.

Hirose, K., 2022. Ten years of investigations of Fukushima radionuclides in the environment: a review on process studies in environmental compartments. J. Environ. Radioact. https://doi.org/10.1016/j.jenvrad.2022.106929.

Igarashi, J., Zheng, J., Zhang, Z., Ninomiya, K., Satou, Y., Fukuda, M., Ni, Y., Aono, T., Shinohara, A., 2019. First determination of Pu isotopes (239Pu, 240Pu and 241Pu) in radioactive particles derived from Fukushima Daiichi Nuclear Power Plant accident. Sci. Rep. 9, 11807 https://doi.org/10.1038/s41598-019-48210-4.

Jaegler, H., Pointurier, F., Diez-Fernández, S., Gourgiotis, A., Isnard, H., Hayashi, S., Tsuji, H., Onda, Y., Hubert, A., Laceby, J.P., Evrard, O., 2019. Reconstruction of uranium and plutonium isotopic signatures in sediment accumulated in the Mano

Dam reservoir, Japan, before and after the Fukushima nuclear accident. Chemosphere 225, 849–858. https://doi.org/10.1016/j.chemosphere.2019.03.064.
Jaegler, H., Pointurier, F., Onda, Y., Hubert, A., Laceby, J.P., Cirella, M., Evrard, O., 2018. Plutonium isotopic signatures in soils and their variation (2011-2014) in sediment transiting a coastal river in the Fukushima Prefecture, Japan. Environ. Pollut. 240, 167–176. https://doi.org/10.1016/j.envpol.2018.04.094.
Japanese Metereological Agency, 2021. Automated Meteorological Data Acquisition System (AMeDAS) Dailly Rain Fall from 2011 to 2021 at Iitate Station.
JAXA, 2022. High-Resolution Land-Use and Land-Cover Map of Japan Ver, 21.11 [2018 ~ 2020] (10 m res.). [WWW Document]. URL. https://earth.jaxa.jp/en/data/2562/index.html. accessed 9.26.22.
Johansen, M.P., Anderson, D., Child, D., Hotchkis, M.A.C., Tsukada, H., Okuda, K., Hinton, T.G., 2021. Differentiating Fukushima and Nagasaki plutonium from global fallout using 241Pu/239Pu atom ratios: Pu vs. Cs uptake and dose to biota. Sci. Total Environ. 754, 141890 https://doi.org/10.1016/j.scitotenv.2020.141890.
Kato, H., Onda, Y., 2018. Determining the initial Fukushima reactor accident-derived cesium-137 fallout in forested areas of municipalities in Fukushima Prefecture. J. For. Res. 23, 1–12. https://doi.org/10.1080/13416979.2018.1448566.
Kelley, J.M., Bond, L.A., Beasley, T.M., 1999. Global distribution of Pu isotopes and 237Np. Sci. Total Environ. 237–238, 483–500. https://doi.org/10.1016/S0048-9697(99)00160-6.
Kersting, A.B., 2013. Plutonium transport in the environment. Inorg. Chem. 52, 3533–3546. https://doi.org/10.1021/ic3018908.
Kitamura, A., Yamaguchi, M., Kurikami, H., Yui, M., Onishi, Y., 2014. Predicting sediment and cesium-137 discharge from catchments in eastern Fukushima. Anthropocene 5, 22–31. https://doi.org/10.1016/j.ancene.2014.07.001.
Kurihara, E., Takehara, Masato, Suetake, M., Ikehara, R., Komiya, T., Morooka, K., Takami, R., Yamasaki, S., Ohnuki, T., Horie, K., Takehara, Mami, Law, G.T.W., Bower, W., Mosselmans, W., J F Warnicke, P., Grambow, B., Ewing, R.C., Utsunomiya, S., 2020. Particulate plutonium released from the Fukushima Daiichi meltdowns. Sci. Total Environ. 743, 140539 https://doi.org/10.1016/j.scitotenv.2020.140539.
Laceby, J.P., Chartin, C., Evrard, O., Onda, Y., Garcia-Sanchez, L., Cerdan, O., 2016a. Rainfall erosivity in catchments contaminated with fallout from the Fukushima Daiichi nuclear power plant accident. Hydrol. Earth Syst. Sci. 20, 2467–2482. https://doi.org/10.5194/hess-20-2467-2016.
Laceby, J.P., Huon, S., Onda, Y., Vaury, V., Evrard, O., 2016b. Do forests represent a long-term source of contaminated particulate matter in the Fukushima Prefecture? J. Environ. Manag. 183, 742–753. https://doi.org/10.1016/j.jenvman.2016.09.020.
Lamb, A.L., Wilson, G.P., Leng, M.J., 2006. A review of coastal palaeoclimate and relative sea-level reconstructions using d13C and C/N ratios in organic material. Earth Sci. Rev. 29–57. https://doi.org/10.1016/j.earscirev.2005.10.003.
Martin, P.G., Griffiths, I., Jones, C.P., Stitt, C.A., Davies-Milner, M., Mosselmans, J.F.W., Yamashiki, Y., Richards, D.A., Scott, T.B., 2016. In-situ removal and characterisation of uranium-containing particles from sediments surrounding the Fukushima Daiichi Nuclear Power Plant. Spectrochim. Acta B Atom Spectrosc. 117, 1–7. https://doi.org/10.1016/j.sab.2015.12.010.
Martin, P.G., Louvel, M., Cipiccia, S., Jones, C.P., Batey, D.J., Hallam, K.R., Yang, I.A.X., Satou, Y., Rau, C., Mosselmans, J.F.W., Richards, D.A., Scott, T.B., 2019. Provenance of uranium particulate contained within Fukushima daiichi nuclear power plant unit 1 ejecta material. Nat. Commun. 10, 1–7. https://doi.org/10.1038/s41467-019-10937-z.
Mathieu, A., Kajino, M., Korsakissok, I., Périllat, R., Quélo, D., Quérel, A., Saunier, O., Sekiyama, T.T., Igarashi, Y., Didier, D., 2018. Fukushima Daiichi–derived radionuclides in the atmosphere, transport and deposition in Japan: a review. Appl. Geochem. 91, 122–139. https://doi.org/10.1016/j.apgeochem.2018.01.002.
Men, W., Zheng, J., Wang, H., Ni, Y., Aono, T., Maxwell, S.L., Tagami, K., Uchida, S., Yamada, M., 2018. Establishing rapid analysis of Pu isotopes in seawater to study the impact of Fukushima nuclear accident in the Northwest Pacific. Sci. Rep. 8, 1892. https://doi.org/10.1038/s41598-018-20151-4.
MEXT, 2011. Results of the Fourth Airborne Monitoring Survey by MEXT.
Ministry of Environment, 2018. Environmental Remediation in Japan March 2018 33.
Misonou, T., Nakanishi, T., Tsuruta, T., Shiribiki, T., Sanada, Y., 2022. Migration processes of radioactive cesium in the Fukushima nearshore area: impacts of riverine input and resuspension. Mar. Pollut. Bull. 178 https://doi.org/10.1016/j.marpolbul.2022.113597.
Muramatsu, Y., Hamilton, T., Uchida, S., Tagami, K., Yoshida, S., Robison, W.L., 2001. Measurement of 240Pu_239Pu isotopic ratios in soils from the Marshall Islands using ICP-MS. Sci. Total Environ. 278, 151–159, 0048-9697/01/$.
Nakanishi, T., Funaki, H., Sakuma, K., 2021. Factors affecting 137Cs concentrations in river water under base-flow conditions near the Fukushima Dai-ichi Nuclear Power Plant. J. Radioanal. Nucl. Chem. 328, 1243–1251. https://doi.org/10.1007/s10967-021-07735-7.
Nishihara, K., Iwamoto, H., Suyama, K., 2012. Estimation of fuel compositions in Fukushima-Daiichi nuclear power plant 202. JAEA.Data/Code/2012-018.
Ochiai, A., Imoto, J., Suetake, M., Komiya, T., Furuki, G., Ikehara, R., Yamasaki, S., Law, G.T.W., Ohnuki, T., Grambow, B., Ewing, R.C., Utsunomiya, S., 2018. Uranium dioxides and debris fragments released to the environment with cesium-rich microparticles from the Fukushima daiichi nuclear power plant. Environ. Sci. Technol. 52, 2586–2594. https://doi.org/10.1021/acs.est.7b06309.
Oikawa, S., Watabe, T., Takata, H., Misonoo, J., Kusakabe, M., 2015. Plutonium isotopes and 241Am in surface sediments off the coast of the Japanese islands before and soon after the Fukushima Dai-ichi nuclear power plant accident. J. Radioanal. Nucl. Chem. 303, 1513–1518. https://doi.org/10.1007/s10967-014-3530-2.
Onda, Y., Taniguchi, K., Yoshimura, K., Kato, H., Takahashi, J., Wakiyama, Y., Coppin, F., Smith, H., 2020. Radionuclides from the Fukushima daiichi nuclear power plant in terrestrial systems. Nat. Rev. Earth Environ. 1, 644–660. https://doi.org/10.1038/s43017-020-0099-x.
R Core Team, 2021. R: A Language and Environment for Statistical Computing. Version 4.1.0. R Foundation for Statistical Computing, Vienna, Austria.
Romanenko, V., Lujanienė, G., 2022. Short review of plutonium applications for the sediment transport studies. J. Environ. Radioact. 257, 107066 https://doi.org/10.1016/j.jenvrad.2022.107066.
Schneider, S., Bister, S., Christl, M., Hori, M., Shozugawa, K., Synal, H.-A., Steinhauser, G., Walther, C., 2017. Radionuclide pollution inside the Fukushima Daiichi exclusion zone, part 2: forensic search for the "Forgotten" contaminants Uranium-236 and plutonium. Applied Geochemistry, Transformation and Fate of Natural and Anthropogenic Radionuclides in the Environments 85, 194–200. https://doi.org/10.1016/j.apgeochem.2017.05.022.
Schneider, S., Walther, C., Bister, S., Schauer, V., Christl, M., Synal, H.-A., Shozugawa, K., Steinhauser, G., 2013. Plutonium release from Fukushima Daiichi fosters the need for more detailed investigations. Sci. Rep. 3, 2988. https://doi.org/10.1038/srep02988.
Shinonaga, T., Steier, P., Lagos, M., Ohkura, T., 2014. Airborne Plutonium and non-natural Uranium from the Fukushima DNPP found at 120 km distance a few days after reactor hydrogen explosions. Environ. Sci. Technol. 48, 3808–3814. https://doi.org/10.1021/es404961w.
Steinhauser, G., Brandl, A., Johnson, T.E., 2014. Comparison of the Chernobyl and Fukushima nuclear accidents: a review of the environmental impacts. Sci. Total Environ. 800–817. https://doi.org/10.1016/j.scitotenv.2013.10.029, 470–471.
Steinhauser, G., Niisoe, T., Harada, K.H., Shozugawa, K., Schneider, S., Synal, H.-A., Walther, C., Christl, M., Nanba, K., Ishikawa, H., Koizumi, A., 2015. Post-accident sporadic releases of airborne radionuclides from the Fukushima daiichi nuclear power plant site. Environ. Sci. Technol. 49, 14028–14035. https://doi.org/10.1021/acs.est.5b03155.
Wei, T., Simko, V., 2021. R Package "Corrplot": Visualization of a Correlation Matrix, Version 0.92.
Wu, J., Zheng, X., Chen, J., Yang, G., Zheng, J., Aono, T., 2022. Distributions and impacts of plutonium in the environment originating from the Fukushima Daiichi Nuclear Power Plant accident: an overview of a decade of studies. J. Environ. Radioact. 248, 106884 https://doi.org/10.1016/j.jenvrad.2022.106884.
Xu, Y., Pan, S., Wu, M., Zhang, K., Hao, Y., 2017. Association of Plutonium isotopes with natural soil particles of different size and comparison with 137Cs. Sci. Total Environ. 581, 541–549. https://doi.org/10.1016/j.scitotenv.2016.12.162. –582.
Yamada, S., Kitamura, A., Kurikami, H., Yamaguchi, M., Malins, A., Machida, M., 2015. Sediment and ^{137} Cs transport and accumulation in the Ogaki dam of eastern Fukushima. Environ. Res. Lett. 10, 014013 https://doi.org/10.1088/1748-9326/10/1/014013.
Yamamoto, M., Hoshi, M., Takada, J., Oikawa, S., Yoshikawa, I., Takatsuji, T., Sekerbaev, A.K., Gusev, B.I., 2002. Some aspects of environmental radioactivity around the former Soviet Union's Semipalatinsk nuclear test site: local fallout Pu in Ust'-Kamenogorsk district. J. Radioanal. Nucl. Chem. 22.
Yamamoto, M., Sakaguchi, A., Ochiai, S., Takada, T., Hamataka, K., Murakami, T., Nagao, S., 2014. Isotopic Pu, Am and Cm signatures in environmental samples contaminated by the Fukushima dai-ichi nuclear power plant accident. J. Environ. Radioact. 132, 31–46. https://doi.org/10.1016/j.jenvrad.2014.01.013.
Yang, G., Tazoe, H., Hayano, K., Okayama, K., Yamada, M., 2017. Isotopic compositions of 236U, 239Pu, and 240Pu in soil contaminated by the Fukushima daiichi nuclear power plant accident. Sci. Rep. 7, 13619 https://doi.org/10.1038/s41598-017-13998-6.
Zheng, J., Tagami, K., Uchida, S., 2013. Release of plutonium isotopes into the environment from the Fukushima daiichi nuclear power plant accident: what is known and what needs to Be known. Environ. Sci. Technol. 47, 9584–9595. https://doi.org/10.1021/es402212v.
Zheng, J., Tagami, K., Watanabe, Y., Uchida, S., Aono, T., Ishii, N., Yoshida, S., Kubota, Y., Fuma, S., Ihara, S., 2012. Isotopic evidence of plutonium release into the environment from the Fukushima DNPP accident. Sci. Rep. 2, 304. https://doi.org/10.1038/srep00304.